Structure–Bioactivity Relationship in Copper(II) Complexes with New Halogenated Coumarin Derivatives[1]

JAKUB KURJAN[1], ZUZANA JENDŽELOVSKÁ[2], VIKTÓRIA DEČMANOVÁ[2], RASTISLAV JENDŽELOVSKÝ[2], NIKOLINA KASTRATOVIC[3], VLADISLAV VOLAREVIC[3], LUKÁŠ SMOLKO[4], ROMANA SMOLKOVÁ[5], MIROSLAVA LITECKÁ[6], ANTON ZUBRIK[7], DÁVID JÁGER[7], RASTISLAV VARHAČ[8], IVAN POTOČŇÁK[1]*

[1]Department of Inorganic Chemistry, Faculty of Science, Pavol Jozef Šafárik University in Košice, Moyzesova 11, 041 54 Košice, Slovakia

[2]Department of Cell Biology, Faculty of Science, Pavol Jozef Šafárik University in Košice, Šrobárova 2, 041 54 Košice, Slovakia

[3]Departments for Genetics, Microbiology and Immunology, Center for Research on Harmful Effects of Biological and Chemical Hazards, Faculty of Medical Sciences, University of Kragujevac, 69 Svetozar Markovic Street, 34000 Kragujevac, Serbia

[4]Department of Medical and Clinical Biochemistry, Faculty of Medicine, Pavol Jozef Šafárik University in Košice, Tr. SNP 1, 040 11 Košice, Slovakia

[5]Center for Applied Biomedicine, Technology and Innovation Park, Pavol Jozef Šafárik University in Košice, Tr. SNP 1, 040 11 Košice, Slovakia

[6]Department of Materials Chemistry, Institute of Inorganic Chemistry of the Czech Academy of Sciences, Husinec-Řež 1001, 250 68 Řež, Czech Republic

[7]Institute of Geotechnics, Slovak Academy of Sciences, Watsonova 45, 040 01 Košice, Slovakia

[8]Department of Biochemistry, Faculty of Science, Pavol Jozef Šafárik University in Košice, Moyzesova 11, 041 54 Košice, Slovakia

Supplementary information

1. Physical measurements

Elemental analyses of C, H, and N were obtained on CHNOS Elemental Analyzer vario MICRO from Elementar Analysensysteme GmbH, Langenselbold, Germany.

[1] Published in the series „Low-dimensional compounds containing bioactive ligands“ as Part XXVII.

The infrared spectra of the prepared compounds were recorded on a Nicolet 6700 FT-IR spectrophotometer from Thermo Scientific equipped with a diamond crystal Smart Orbit™ in the range 4000-400 cm^{-1}. To process the results, the program OMNIC™ from Thermo Scientific was used.

Absorption spectra were measured with a SPECORD 250 spectrophotometer (Analytik Jena, Jena, Germany), from 450 to 900 nm, in Nujol, DMSO, and DMSO/water (1:1) solutions at 24, 48 and 72 h intervals.

NMR spectra were recorded on a Varian VNMRS (599.87 MHz for ^{1}H and 150.84 MHz for ^{13}C) spectrometer with a 5-mm inverse-detection H-X probe equipped with a z-gradient coil at 299.15 K. All the pulse programs were taken from the Varian sequence library. Chemical shifts (*d* in ppm) are given from internal solvent and the partially deuterated residual DMSO-d_6 39.5 ppm for ^{13}C; DMSO-d_5 2.5 ppm for ^{1}H. NMR spectra were processed and analyzed in MestReNova v. 14.3.3 (Mestrelab Research, Spain).

1.1. X-ray data collection and structure refinement

The data collection for **5** was carried out on an XtaLAB Synergy diffractometer equipped with a HyPix detector. The data collections for **6-9** were carried out on an Oxford Diffraction Xcalibur2 diffractometer equipped with a Sapphire2 CCD detector. CrysAlisPro [1] software was used for data collection and cell refinement, data reduction, and absorption correction. The structures were solved by SHELXT [2] and refined by subsequent Fourier syntheses using SHELXL-2018 [3], implemented in WinGX program suit [4]. Carbon-bonded hydrogen atoms were placed in calculated positions and refined riding on their parent C atoms. Nitrogen-bonded hydrogen atoms were found in the difference Fourier maps and then refined riding on their parent N atoms. A geometric analysis was performed using SHELXL-2018, PLATON [5] was used to analyze π-π interactions, while DIAMOND [6] was used for molecular graphics.

1.2. Mass spectrometry

Mass spectrometry was performed using a Bruker Compact Q-TOF (quadrupole-time of flight) hybrid mass spectrometer (Bruker Daltonics, Bremen, Germany) equipped with an ESI (electrospray ionization) source operated in negative mode. Samples were dissolved in methanol and introduced via direct injection into the mass spectrometer. External calibration was performed using sodium formate clusters. The accurate masses of the molecular and fragment ions from the MS/MS experiments were used to determine empirical formulas and to propose structure of Cu(II) complexes. The mass deviations (experimental vs. theoretical) for all *m*/*z* values were < 5 ppm.

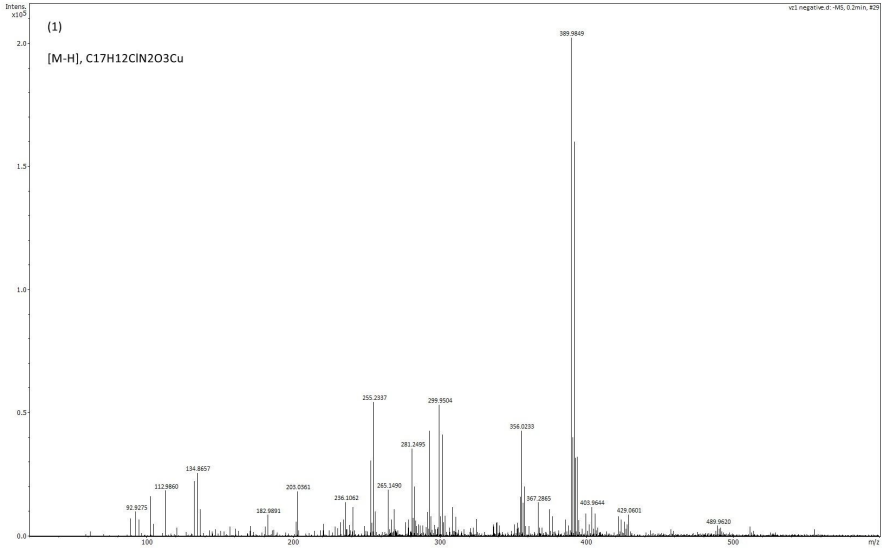
(1)
[M-H], C17H12ClN2O3Cu
vc1 negative.d: -MS, 0.2min, #29
Intens.
x10^5
389.9849
255.2337
299.9504
356.0233
281.2495
134.8657
112.9860
265.1490
236.1062
205.0561
367.2865
403.9644
429.0601
92.9275
182.9891
489.9620
m/z

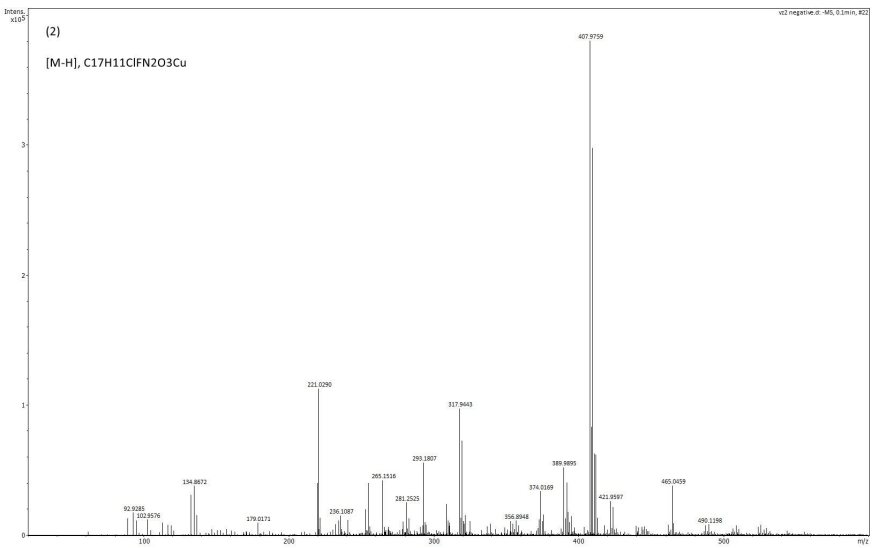
(2)
[M-H], C17H11ClFN2O3Cu
vc2 negative.d: -MS, 0.1min, #22
Intens.
x10^5
407.9759
221.0290
317.9443
293.1807
134.8672
265.1516
281.2525
389.9895
374.0169
465.0459
421.9597
92.9265
102.9576
179.0171
236.1087
356.8948
490.1198
m/z

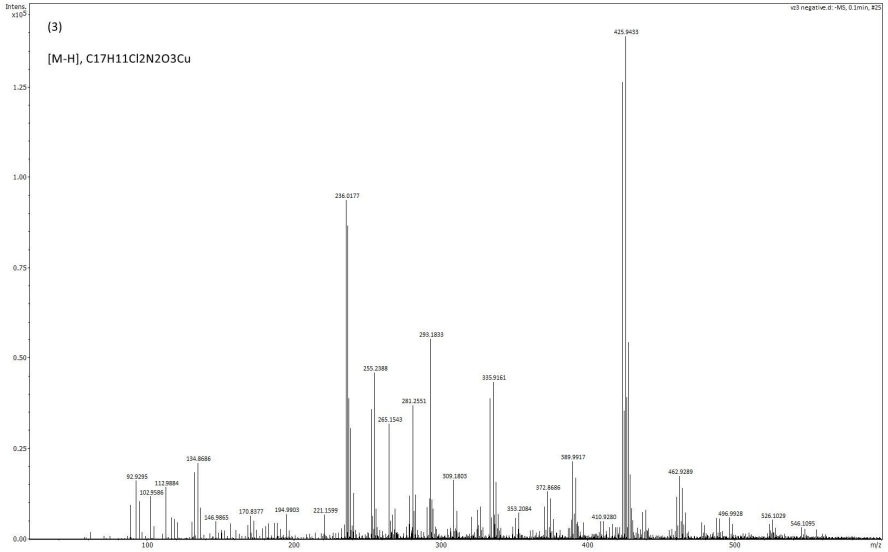
(3)
[M-H], C17H11Cl2N2O3Cu
vc3 negative.d: -MS, 0.1min, #25
Intens.
x10^5
425.9433
236.0177
293.1833
255.2388
335.9161
281.2551
265.1543
134.8686
92.9295
112.9884
102.9586
309.1805
389.9917
372.8686
462.9289
146.9865
170.8377
194.9903
221.1599
353.2084
410.9280
496.9928
526.1029
546.1095
m/z

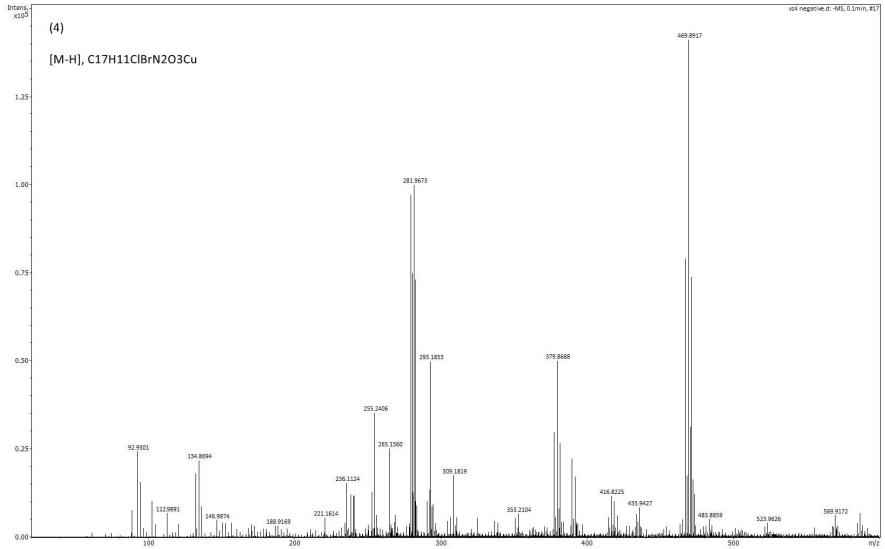
(4)
[M-H], C17H11ClBrN2O3Cu
vc4 negative.d: -MS, 0.1min, #17
Intens.
x10^5
469.8917
281.9673
295.1853
379.8688
253.2406
265.1560
92.9301
154.8694
236.1124
309.1819
416.8225
433.9427
112.9891
146.9874
188.9169
221.1614
353.2104
485.8859
523.9626
569.9172
m/z

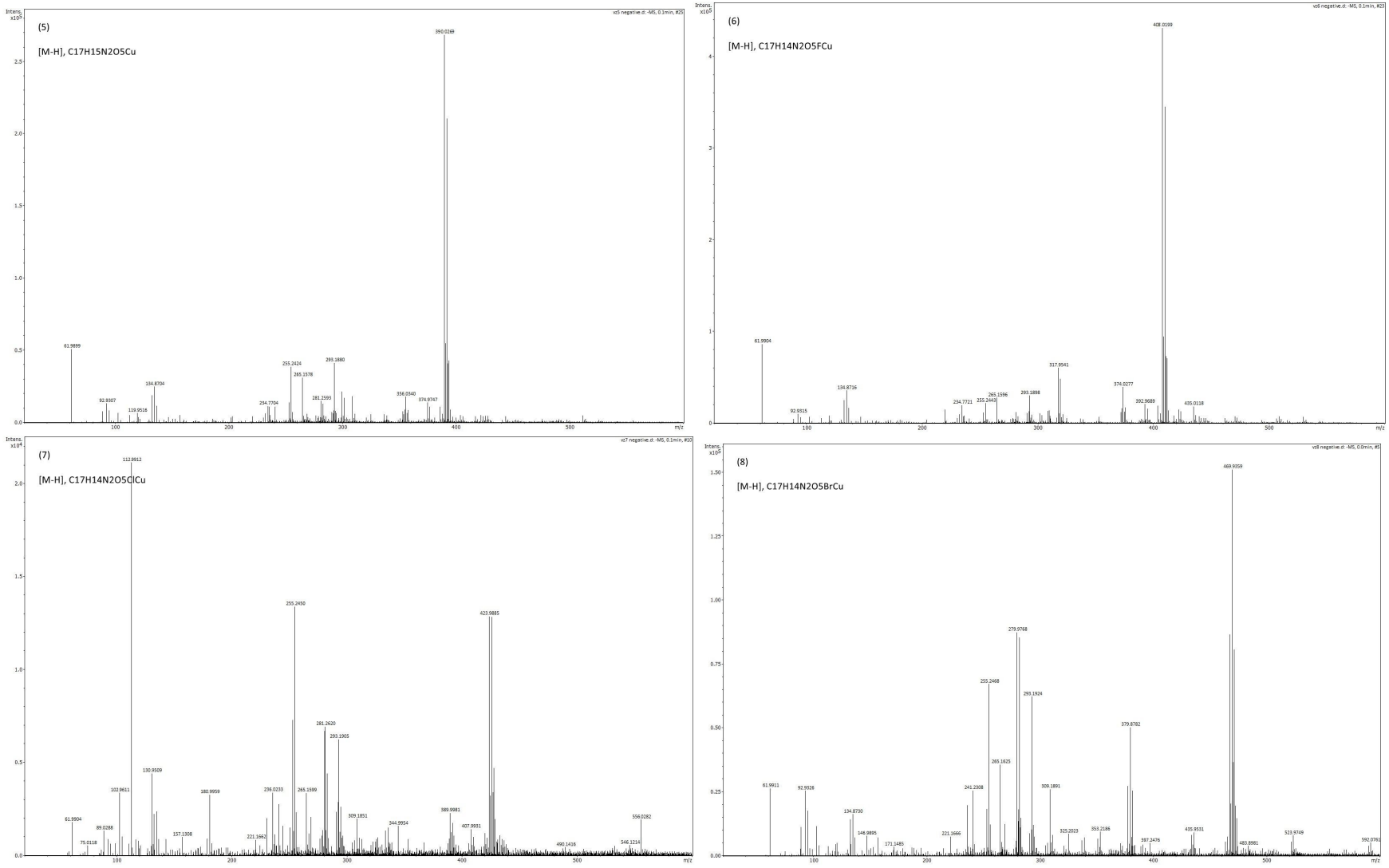

Figure S1. ESI-MS analysis of compounds **1**–**8**. Theoretical and measured masses of first peak of isotope cluster (monoisotopic mass) and proposed formulas are listed in Table 2.

2. Cell cultures

For MTT assay and IC_{50} evaluation, MDA-MB-231 breast cancer cells were obtained from the American Type Culture Collection (ATCC, Manassas, VA, USA). HCT 116 colorectal cancer cells and periodontal ligament-derived mesenchymal stem cells (PDL-MSCs) were generously supplied by Dr. Danijela Vignjević (Institut Curie, Paris, France) and Dr. Olivera Milošević Đorđević (University of Kragujevac, Serbia), respectively. All cell lines were cultured in Dulbecco's Modified Eagle Medium (DMEM; Sigma-Aldrich, Munich, Germany) supplemented with 10% fetal bovine serum (FBS; Sigma), 100 IU/mL of penicillin, and 100 µg/mL of streptomycin. Cultures were maintained at 37 °C in a humidified incubator with 5% CO_2 and 95% air. Cell viability and counts were assessed using trypan blue exclusion staining.

For cell proliferation assay, quantification of cell number and viability, cell cycle analysis, and phosphatidylserine externalisation analysis, human colorectal adenocarcinoma cell line HCT 116 and human breast adenocarcinoma cell line MDA-MB-231 were used. Both cell lines were purchased from the American Type Culture Collection (ATCC). HCT 116 cells were cultured in McCoy's 5A medium (PAN-Biotech GmbH, Aidenbach, Germany) and MDA-MB-231 cells were cultured in complete RPMI-1640 medium (Sigma-Aldrich), both in an incubator at 37 °C with 5% CO_2 and 95% humidity. All culture media were supplemented with 10% fetal bovine serum (FBS; Biosera, Nuaillé, France), 7.5% $NaHCO_3$, and antibiotics (1% antibiotic–antimycotic 100 × and 50 µg/mL gentamicin; Biosera).

2.1. Inhibitory effect testing

The inhibitory potential of the compounds was evaluated using the MTT colorimetric assay. MDA-MB-231, HCT 116, and PDL-MSCs cells were diluted in RPMI 1640 medium to a concentration of 5×10^4 cells/mL. Aliquots of 5×10^3 cells in 100 µL were seeded into individual wells of 96-well plates. After 24 h, the medium was replaced with 100 µL of test compounds, prepared by serial two-fold dilution to yield final concentrations ranging from 500 µM to 3.9 µM in RPMI medium. Each condition was tested in triplicate.

Cells were incubated for 72 h at 37 °C in a 5% CO_2 atmosphere. Post-incubation, the medium was discarded, and 10 µL of MTT solution (5 mg/mL in PBS) was added to each well. Following an additional 4-h incubation, the MTT-containing medium was removed, and 150 µL of DMSO along with 20 µL of glycine buffer was added to dissolve the formazan crystals. The plates were shaken for 10 minutes, and absorbance was measured at 595 nm using a microplate reader.

Inhibitory effect was calculated using the equation 1:

$$\%\ Inhibitory\ effect = \frac{100 - ((TS - BG_0) - E)}{(TS - BG_0)} \times 100 \quad \text{(eq. 1)}$$

where BG_0 represents the background absorbance from medium-only wells, *TS* denotes total survival/spontaneous death of untreated control cells, and *E* refers to the absorbance from experimental wells.

2.2. *In vitro* antitumor activity

2.2.1. Reagents

For evaluation of *in vitro* antitumor activity, all tested chemicals were freshly prepared before each experiment. Copper salts $CuCl_2$ and $Cu(NO_3)_2$, as well as prepared complexes **3**, **4**, and **7** were dissolved in dimethyl sulfoxide (DMSO) to a final concentration of 10 mM. Stock solutions were stored at room temperature in the dark and diluted in culture medium to working concentrations immediately prior to the addition to the cell cultures. Cisplatin (CDDP; cis-diamminedichloridoplatinum; CAS No.: 15663-27-1), used as a reference antineoplastic drug, was manufactured by EBEWE Pharma GmbH Nfg KG (Unterach, Austria) as an aqueous solution (0.5 mg/mL). It was also freshly diluted in culture medium to the appropriate working concentrations before being added to the cells.

2.2.2. Cell proliferation assay

For the cell proliferation assay, HCT 116 and MDA-MB-231 cells were seeded into 96-well plates (TPP, Trasadingen, Switzerland) at a density of 7,000 and 10,000 cells per well, respectively, and allowed to adhere for 24 h prior to treatment. Subsequently, the cells were treated with different concentrations of complexes **3**, **4**, **7**, CDDP, $CuCl_2$, and $Cu(NO_3)_2$ ranging from 1 μM to 50 μM, or with 0.5% DMSO (the highest final DMSO concentration corresponding to the concentration in the experimental groups treated with 50 μM of tested complexes).

To assess the potential antiproliferative (cytostatic) effects of tested compounds on HCT 116 and MDA-MB-231 cells, a real-time label-free proliferation assay was performed using the IncuCyte™ ZOOM live cell imaging system (Essen BioScience, Ann Arbor, MI, USA). Immediately after treatment, the 96-well plates were placed into the IncuCyte™ ZOOM system located inside a standard humidified cell culture incubator (37 °C, 5% CO_2, 95% humidity). Cell proliferation was monitored by measuring confluence as the percentage of the well surface area covered by cells every 2 h for a total duration of 72 h using the IncuCyte™ ZOOM automated software (IncuCyte™ ZOOM 2016B). Results were expressed as percentages of confluence in untreated controls and treated experimental groups.

2.2.3. Quantification of cell number and viability

To assess total cell number and viability in each experimental group, HCT 116 and MDA-MB-231 cells were seeded into 6-well plates (TPP) at densities of 150,000 and 220,000 cells per well, respectively, and allowed to adhere for 24 h prior to treatment. Subsequently, the cells were treated with 7.5 μM or 12.5 μM of complexes **3**, **4**, and **7**, and CDDP, or with 12.5 μM of $CuCl_2$ and $Cu(NO_3)_2$. The total cell population (floating and adherent cells) was harvested 48 h after the treatment by trypsinization and counted using a Vi-CELL XR Cell Viability Analyzer (Beckman Coulter, Indianapolis, IN, USA) immediately after vital staining with trypan blue. Total cell number was expressed as a percentage of the untreated control. Viability was expressed as a percentage of viable cells within the total cell population.

2.2.4. Flow cytometry analyses

To investigate the potential cytotoxic and/or cytostatic effects of selected complexes, flow cytometric analyses of phosphatidylserine externalization and cell cycle distribution were performed. HCT 116 and MDA-MB-231 cells were seeded into 6-well plates (TPP) at densities of 150,000 and 220,000 cells per well, respectively, and allowed to adhere for 24 h prior to treatment. Subsequently, the cells were treated with 7.5 μM or 12.5 μM of complexes **3**, **4**, and **7**, and CDDP, or with 12.5 μM of $CuCl_2$ and $Cu(NO_3)_2$. The total cell population (floating and adherent cells) was harvested 48 h after the treatment by trypsinization, centrifuged, washed with PBS, and divided for subsequent flow cytometry analyses.

2.2.4.1. Cell cycle analysis

For cell cycle analysis, the cells were centrifuged, fixed in cold 70% ethanol and kept at −20 °C overnight. Prior to analysis, cells were washed twice with PBS, resuspended in the staining solution (0.1% Triton X-100, 0.137 mg/mL ribonuclease A and 0.02 mg/mL propidium iodide – PI) and incubated in the dark at room temperature for 30 min. Samples (15×10^3 cells per sample) were analyzed using a BD FACSAria II SORP flow cytometer (BD Biosciences, San Jose, CA, USA) with a 488 nm blue excitation laser. Fluorescence was detected via a PE-Texas Red (DM600LP-610/20) emission filter. ModFit 3.3 software (Verity Software House, Topsham, ME, USA) was used to generate DNA content frequency histograms and quantify the distribution of cells in the individual cell cycle phases. Results are expressed as percentages of the cells in G0/G1, S and G2/M phases of the cell cycle.

2.2.2.5. Phosphatidylserine externalization analysis

For phosphatidylserine externalization and cell death analysis, a BD Pharmingen FITC Annexin V Apoptosis Detection Kit I (BD Biosciences) was used according to the manufacturer´s instructions. The cells were centrifuged, washed with Hank's balanced salt solution (HBSS) and stained with Annexin V-FITC in 1 × binding buffer for 15 min at 37 °C in the dark. Prior to analysis by BD FACSAria II SORP flow cytometer (BD Biosciences), cells were stained with PI (1 μg/mL). Fluorescence was

detected via a FITC (DM505LP-525/50; Annexin V-FITC) and a PE (DM550LP-575/25; PI) emission filters. The results were analyzed using FlowJo software (Tree Star Inc., Ashland, OR, USA) and were expressed as percentages of early apoptotic cells (Annexin V^+/PI^-), late apoptotic cells (Annexin V^+/PI^+), necrotic cells (Annexin V^-/PI^+), and living cells (Annexin V^-/PI^-).

2.2.3.Statistical analyses

The results are expressed as the mean values ± standard deviation (SD) of at least three independent experiments. The data were analyzed using one-way ANOVA with Tukey's post-test and the significance levels are indicated in the legend for each particular figure.

3 Hirshfeld surface analysis

The Hirshfeld surface was calculated using the CrystalExplorer software [7].

4 Radical scavenging activity analysis

Radical scavenging activity of complexes **3**, **4** and **7** was determined by DPPH (2,2-diphenyl-1-picrylhydrazyl; TCI, Japan) radical. It is worth noting that attempts to measure the activity with ABTS radical (diammonium 2,2'-azino-bis(3-ethylbenzothiazoline-6-sulfonate) according to a standard assay led to a precipitation in the solutions, therefore the ABTS assay could not be used for the radical scavenging evaluation. Methanolic solutions of compounds **3**, **4** and **7** (0 – 200 μM) were mixed with a methanolic solution of DPPH. After incubation in the dark at room temperature for 30 min, the absorbance was recorded at 517 nm. The results are expressed as a percentage radical scavenging activity Q values at corresponding concentration of tested compounds according to equation 2:

$$\%\, Q = \frac{(A_0 - A)}{A_0} \times 100 \qquad \text{(eq. 2)}$$

where A_0 and A represent the absorbance in the absence and presence of the tested compounds, respectively. The experiments were carried out in duplicate.

5 DNA and HSA binding analysis

DNA binding studies with ethidium bromide (EB) were carried out by standard fluorescence assay. DNA-EB complex was prepared by mixing solutions of calf thymus DNA (100 ng/μL) with a solution of EB (50 μM). Prepared DNA-EB complex solution was treated with solutions of gradually increasing concentration of respective complexes **3**, **4**, and **7** and the corresponding ligands (0-25 μM). The emission spectra were recorded in the range of 560-700 nm upon excitation at 520 nm. A human serum albumin (HSA) binding study was performed using a standard tryptophan quenching assay. Solutions of complexes **3**, **4**, and **7** and the corresponding ligands (0-0.2 μM) were gradually added to an albumin solution (0.4 μM). The emission spectra were recorded in the 310-500 nm range upon excitation at 295 nm. The strength of binding interactions in DNA and HSA assays was calculated as quenching

percentage and Stern-Volmer binding constants (K_{SV}) according Stern-Volmer equation (eq. 3). Furthermore, HSA assay results were also expressed by number of binding sites n and K_b binding constants calculated according to the modified Stern-Volmer equation (eq. 4) [8].

$$\frac{F_0}{F} = 1 + K_{SV}[Q] \quad \text{(eq. 3)}$$

$$log\frac{F_0 - F}{F} = \log [K_b] + n\log [Q] \quad \text{(eq. 4)}$$

F_0 and F are the emission maxima of EB-DNA or HSA solutions, respectively, in the presence of tested complexes, $[Q]$ is the concentration of tested complexes, K_{SV} and K_b are respective binding constants, and n is the number of binding sites.

6 Viscometry measurement

Viscosity measurements were conducted with a Lovis 2000 M/ME Rolling-Ball Microviscometer at 25 °C. In the experiments short Lovis 1.59 mm capillary was used and viscosity was measured at angle of 25°. The results were plotted as $(\eta/\eta_0)^{1/3}$ against the [compound]/[DNA] ratio, where η and η_0 represent the relative viscosities of DNA in the presence and absence of the complexes, respectively. To elucidate the binding mode of compounds **3**, **4**, and **7**, experiments were performed by maintaining a constant ct-DNA concentration (100 μM) while varying the concentration of the complexes. Each concentration was measured in triplicate, and the median values were used.

7 Lipophilicity measurement

Octanol (99%) and dimethyl sulfoxide (99.59%) were purchased from Merck, Darmstadt, Germany and Lach-Ner, Neratovice, Czech Republic, respectively. A SPECORD 250 spectrophotometer (Analytik Jena, Jena, Germany) was employed to record absorption spectra in the wavelength range of 400–800 nm. Distilled water was saturated with n-octanol, and conversely, n-octanol was saturated with distilled water by vigorous shaking of the biphasic mixtures for 24 h, followed by phase separation over an additional 24 h.

Stock solutions of compounds **3**, **4** and **7** were prepared in DMSO at a concentration of 18.86 mmol. An aliquot of 60 μL of each stock solution was diluted to 2.0 mL with water previously saturated with n-octanol. Subsequently, 2.0 mL of n-octanol was added to each solution of **3**, **4** and **7**, and the resulting biphasic systems were vigorously shaken for 1 h. The mixtures were then allowed to stand for 24 h to ensure complete phase separation.

After phase separation, samples of the aqueous phase from each system were collected and analyzed by UV-Vis spectrophotometry at the respective λ_{max} of compounds **3**, **4** and **7** (Table S1). Each experiment was performed in triplicate, and the median value of the measurements was used for further analysis.

Table S1. λ_{max} and absorbance of compounds **3**, **4** and **7**.

	λ_{max} [nm]	**Absorbance (average value from 3 experiments)**
3	625	0.044195
4	624	0.035533
7	624	0.046055

Calibration (standard) curves for compounds **3**, **4** and **7** were obtained by serial dilution of the corresponding stock solutions. Aliquots of 20, 40, 60, 80 and 100 μL were taken from each stock solution and diluted with distilled water to a final volume of 2.0 mL for UV-Vis spectrophotometric analysis. Using statistical analysis, linear regression equations were derived from the calibration data and applied to determine the unknown concentrations of the analytes in the aqueous phase after partitioning. The logP values were then calculated according to the following equation:

$$logP = log\frac{c_o}{c_w} \qquad \text{(eq. 5)}$$

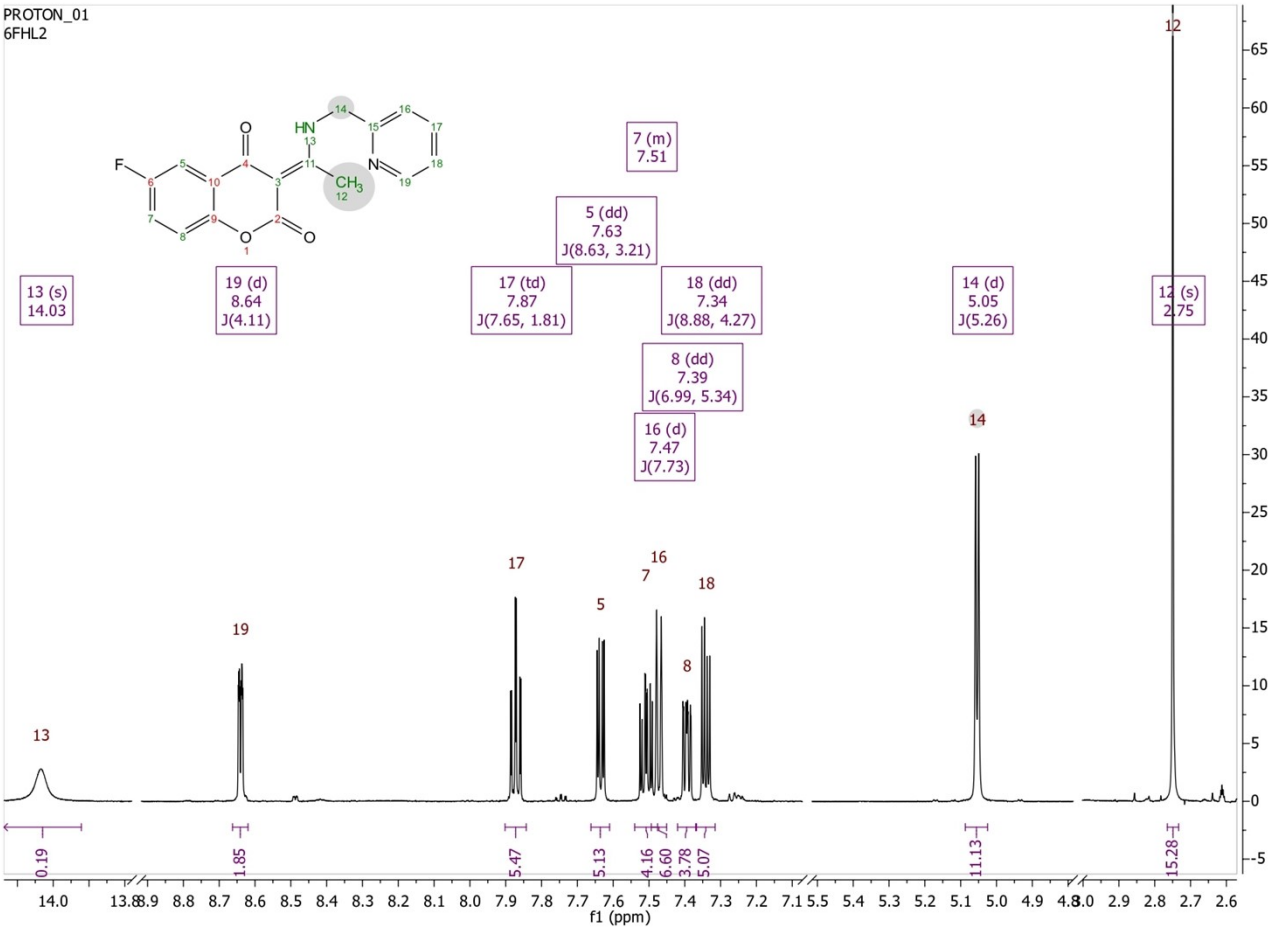

Figure S2. 1H NMR spectrum of **6F-HL**.

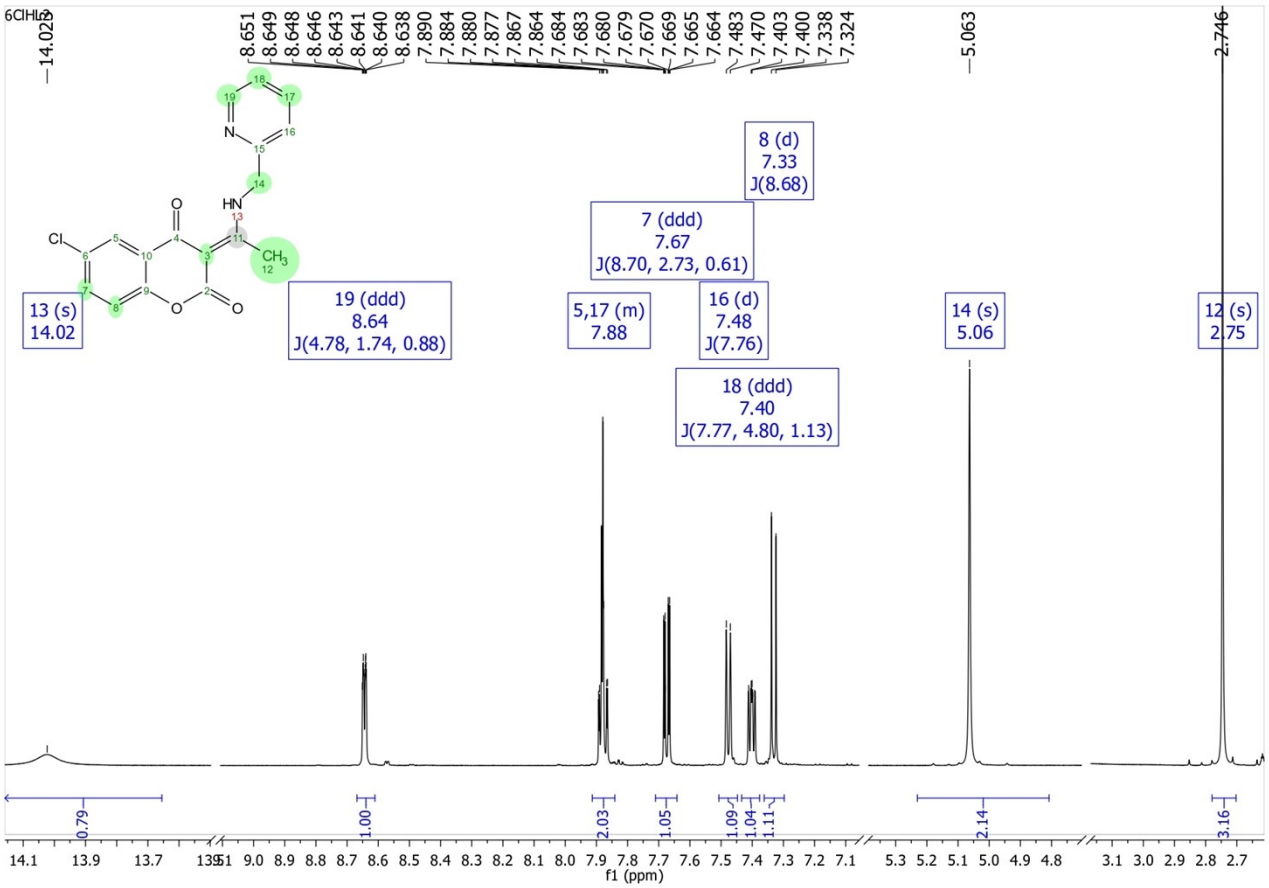

Figure S3. 1H NMR spectrum of **6Cl-HL**.

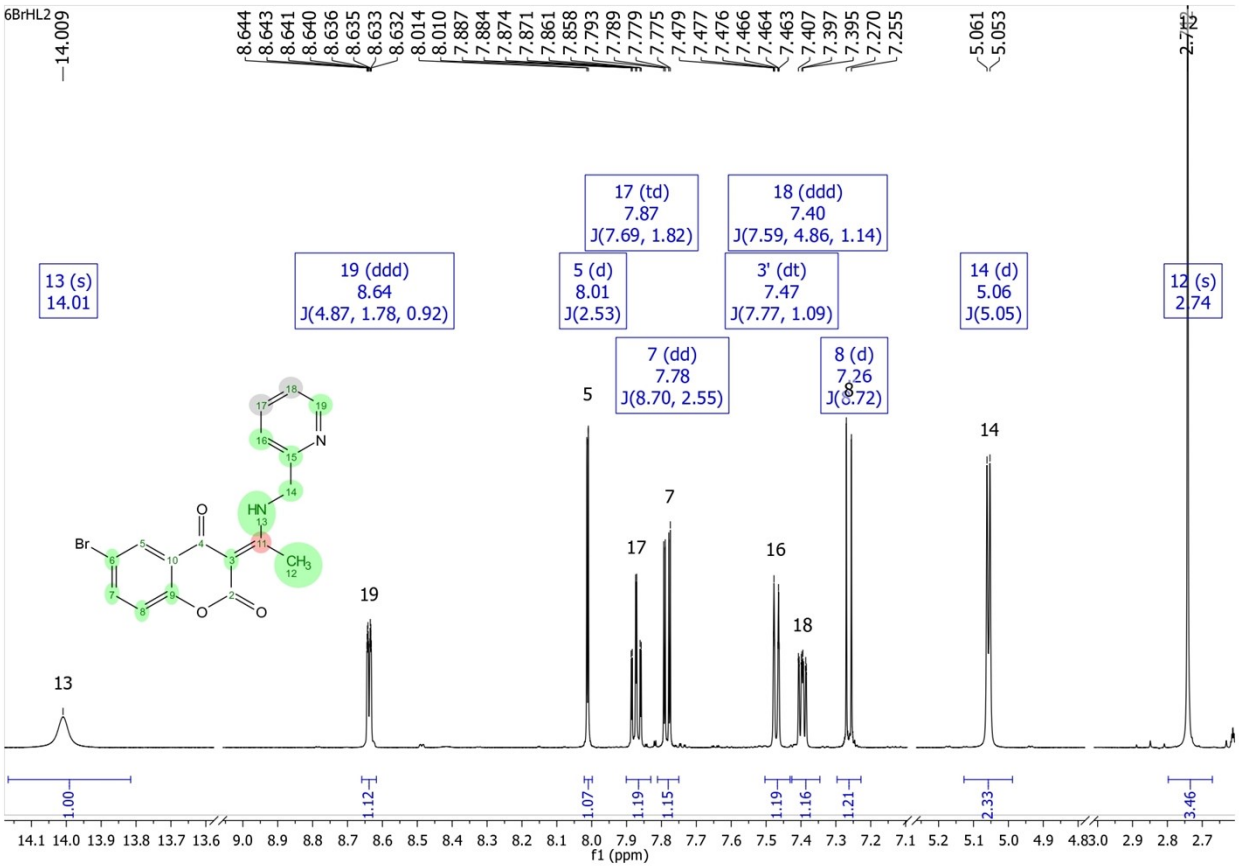

Figure S4. 1H NMR spectrum of **6Br-HL**.

Table S2. Hydrogen bonds [Å, °] in the structures of complexes **5**–**9**.

	D–H···A	***d*(D–H)**	***d*(H···A)**	***d*(D···A)**	**<(DHA)**
5	O40–H40B···O31^{i}	0.85	1.85	2.689(3)	167.3
	O40–H40A···O2^{ii}	0.85	1.93	2.729(3)	155.6
	C19–H19···O21^{ii}	0.95	2.39	3.326(4)	170.0
	C8–H8···O32^{iii}	0.95	2.54	3.457(4)	163.5
	C12–H12B···O2	0.98	2.24	2.695(4)	106.7
	C5–H5···O31^{i}	0.95	2.47	3.366(4)	157.2
	C12–H12C···O33^{iv}	0.98	2.50	3.473(4)	169.5
	C14–H14B···O33^{iv}	0.99	2.48	3.317(4)	141.7
	C17–H17···O32^{v}	0.95	2.52	3.128(4)	122.0

6	C7–H7···O32^{ii}	0.95	2.52	3.161(3)	124.7
	C12–H12A···O2	0.98	2.38	2.849(3)	108.9
	C14–H14A···O2^{iii}	0.99	2.44	3.076(3)	121.5
7	C7–H7···O32^{ii}	0.95	2.43	3.209(3)	138.6
	C12–H12A···O2	0.98	2.34	2.868(3)	112.9
	C14–H14A···O2^{iii}	0.99	2.58	3.204(3)	120.9
8	C7–H7···O32^{ii}	0.95	2.45	3.251(3)	142.4
	C12–H12A···O2	0.98	2.33	2.877(4)	114.1
9	C12–H12A···O2	0.98	2.17	2.737(4)	115.8
	C14–H14A···O3^{iii}	0.99	2.50	3.299(3)	137.9
	C19–H19···O31	0.95	2.58	3.095(4)	114.4
	C12–H12C···O2^{iv}	0.98	2.55	3.179(3)	121.7
	C17–H17···O2^{v}	0.95	2.59	3.188(4)	121.0

5: i = -*x*, -*y* + 1, -*z* + 1; ii = *x*, *y* – 1, *z*; iii = -*x*, -*y* + 2, -*z* + 1; iv = *x* + 1, *y*, *z*; v = -*x* + 1, -*y* + 1, *z*; **6**: ii = -*x* + 1, -*y,* -*z* + 1; iii = -*x* + 3/2, *y* + ½, -*z* + ½; **7**: ii = -*x* + 1, *y* + 2, -*z* + 1; iii = -*x*, *y* – ½, -*z* + ½; **8**: ii = -*x* + 1, -*y* + 2, -*z* + 1; **9**: iii = *x*, *y* – 1, *z*; iv = -*x* + 2, -*y*, -*z* + 1; v = *x* + ½, -*y* + ½, *z* + ½;

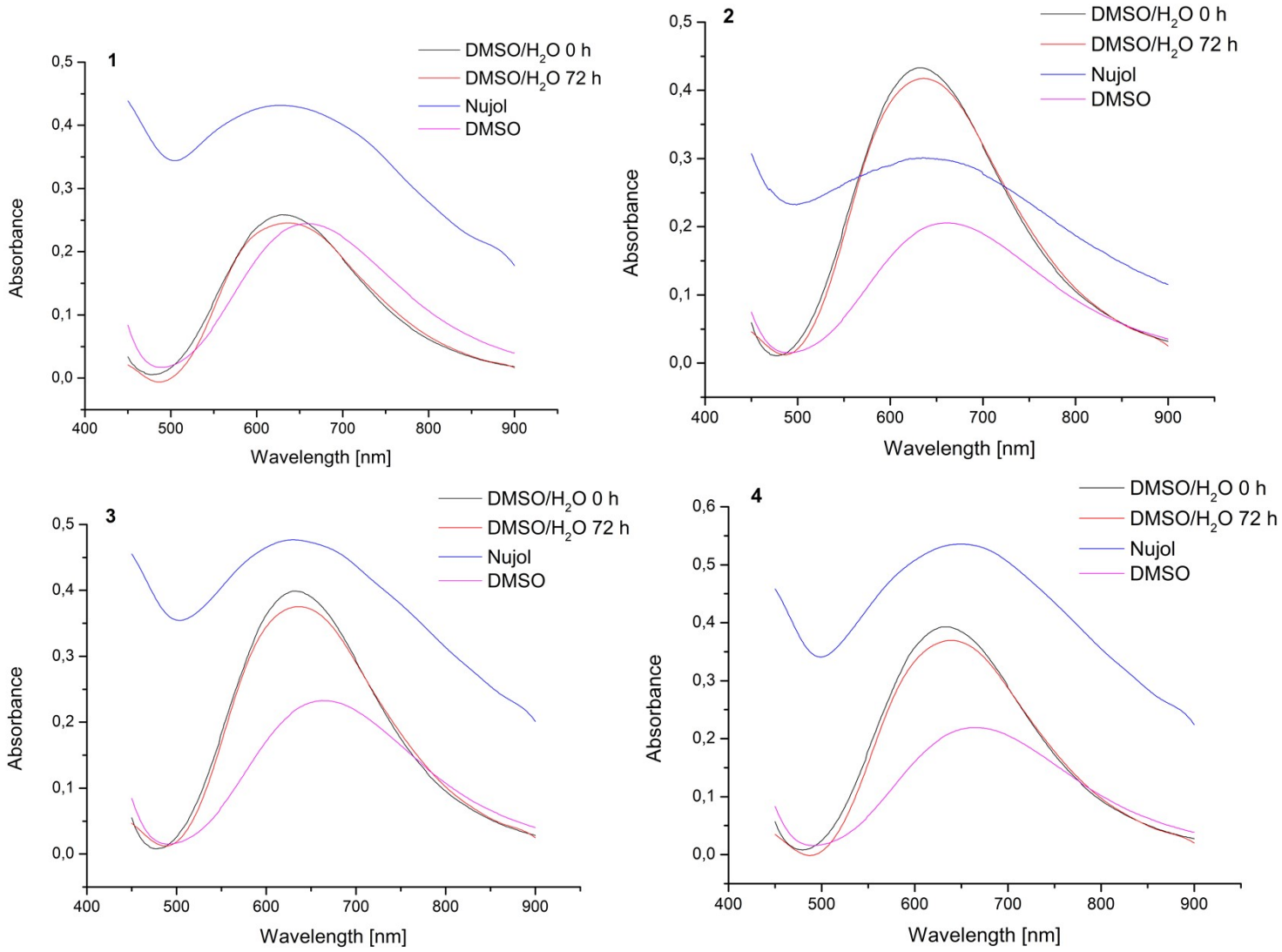
1
DMSO/H2O 0 h
DMSO/H2O 72 h
Nujol
DMSO
Absorbance
Wavelength [nm]
2
DMSO/H2O 0 h
DMSO/H2O 72 h
Nujol
DMSO
Absorbance
Wavelength [nm]
3
DMSO/H2O 0 h
DMSO/H2O 72 h
Nujol
DMSO
Absorbance
Wavelength [nm]
4
DMSO/H2O 0 h
DMSO/H2O 72 h
Nujol
DMSO
Absorbance
Wavelength [nm]

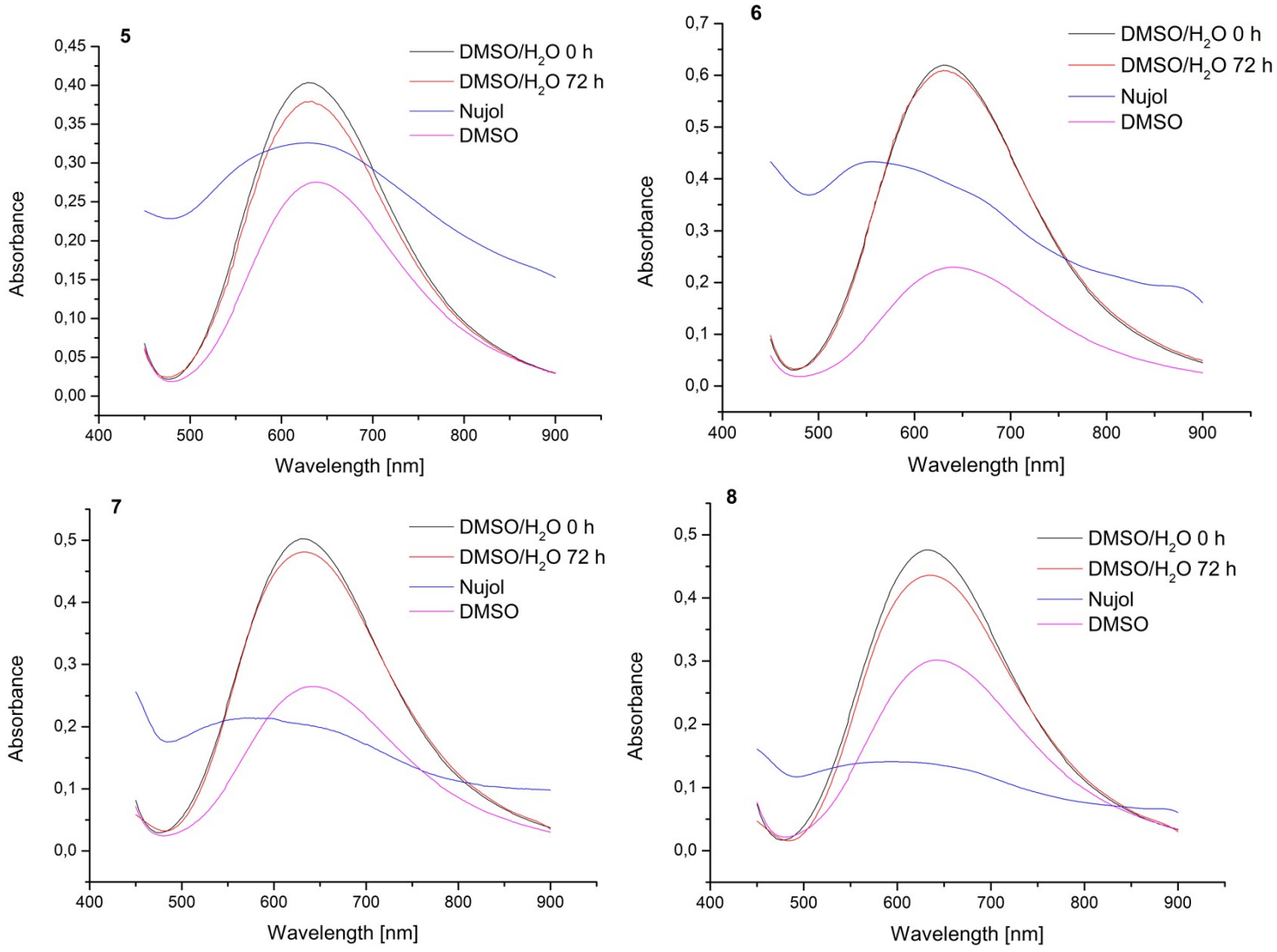
5
DMSO/H2O 0 h
DMSO/H2O 72 h
Nujol
DMSO
Absorbance
Wavelength [nm]
6
DMSO/H2O 0 h
DMSO/H2O 72 h
Nujol
DMSO
Absorbance
Wavelength [nm]
7
DMSO/H2O 0 h
DMSO/H2O 72 h
Nujol
DMSO
Absorbance
Wavelength [nm]
8
DMSO/H2O 0 h
DMSO/H2O 72 h
Nujol
DMSO
Absorbance
Wavelength [nm]

Figure S5. Measurement of stability of complexes **1**–**8** in solution DMSO/water for 72 hours by UV-Vis spectroscopy. Graphs include spectra of **1**–**8** measured in pure DMSO and nujol.

Table S3. Crystal data and structure refinement of **5**–**9**.

	5	**6**	**7**	**8**	**9**
Empirical formula	$C_{17}H_{15}N_3O_7Cu$	$C_{34}H_{24}Cu_2F_2N_6O_{12}$	$C_{34}H_{24}Cl_2Cu_2N_6O_{12}$	$C_{34}H_{24}Br_2Cu_2N_6O_{12}$	$C_{17}H_{12}BrCuN_3O_6$
Formula weight	436.86	873.67	906.57	995.49	497.75
Temperature [K]	100(2)	173(2)	173(2)	173(2)	173(2)
Wavelength [Å]	1.54184	0.71073	0.71073	0.71073	0.71073
Crystal system	Triclinic	Monoclinic	Monoclinic	Monoclinic	Monoclinic
Space group	*P*-1	$P2_1/n$	$P2_1/c$	$P2_1/c$	$P2_1/n$
Unit cell dimensions [Å, °]	a = 8.2150(3)	a = 9.2226(3)	a = 9.1920(3)	a = 9.3394(3)	a = 9.7971(6)
	b = 9.8266(5)	b = 11.4194(4)	b = 11.7488(4)	b = 11.8109(4)	b = 8.3659(4)
	c = 10.9541(3)	c = 16.1604(5)	c = 16.3509(6)	c = 16.5569(6)	c = 21.8709(12)
	α = 85.363(3)				
	β = 84.610(3)	β = 106.219(3)	β = 105.517(4)	β = 105.541(4)	β = 94.624(5)
	γ = 72.071(4)				
Volume [Å^3]	836.35(6)	1634.22(10)	1701.45(11)	1759.56(11)	1786.74(17)
Z; density (calculated) [g.cm^{-3}]	2; 1.735	2; 1.775	2; 1.770	2; 1.879	4; 1.850

Absorption coefficient [mm^{-1}]	2.309	1.392	1.485	3.555	3.501
$F(000)$	446	884	916	988	988
Crystal size [mm^3]	0.207 x 0.073 0.064	0.480 x 0.171 x 0.156	0.595 x 0.222 x 0.164	0.399 x 0.141 x 0.100	0.467 x 0.187 x 0.098
θ range for data collection [°]	4.060 to 77.764	2.911 to 28.792	2.880 to 29.116	2.846 to 28.927	3.069 to 28.809
Index ranges	$-8 \le h \le 10$; $-11 \le k \le 12$; $-13 \le l \le 13$	$-11 \le h \le 12$; $-14 \le k \le 14$; $-21 \le l \le 20$	$-12 \le h \le 12$; $-14 \le k \le 15$; $-22 \le l \le 21$	$-12 \le h \le 12$; $-15 \le k \le 12$; $-22 \le l \le 21$	$-13 \le h \le 9$; $-7 \le k \le 10$; $-28 \le l \le 28$
Reflections collected / independent	9781/3291 [R(int) = 0.0487]	18451/3941 [R(int) = 0.0333]	19563/4122 [R(int) = 0.0382]	9184/3976 [R(int) = 0.0231]	8138/4050 [R(int) = 0.0231]
Data / restraints / parameters	3291 / 0 / 254	3941 / 0 / 254	4122 / 0 / 254	3976 / 0 / 254	4050 / 0 / 254
Goodness-of-fit on F^2	1.091	1.027	1.045	1.025	1.067
Final R indices [$I > 2\sigma(I)$]	$R1$ = 0.0468, $wR2$ = 0.1326	$R1$ = 0.0334, wR2 = 0.0744	$R1$ = 0.0331, $wR2$ = 0.0770	$R1$ = 0.0301, $wR2$ = 0.0722	$R1$ = 0.0333, $wR2$ = 0.0673
R indices (all data)	$R1$ = 0.0511, $wR2$ = 0.1381	$R1$ = 0.0515, wR2 = 0.0828	$R1$ = 0.0473 $wR2$ = 0.0855	$R1$ = 0.0455 $wR2$ = 0.0790	$R1$ = 0.0518 $wR2$ = 0.0747
Largest diff. peak and hole [$e.Å^{-3}$]	0.638 and -0.999	0.431 and -0.365	0.468 and -0.577	0.600 and -0.387	0.714 and -0.390

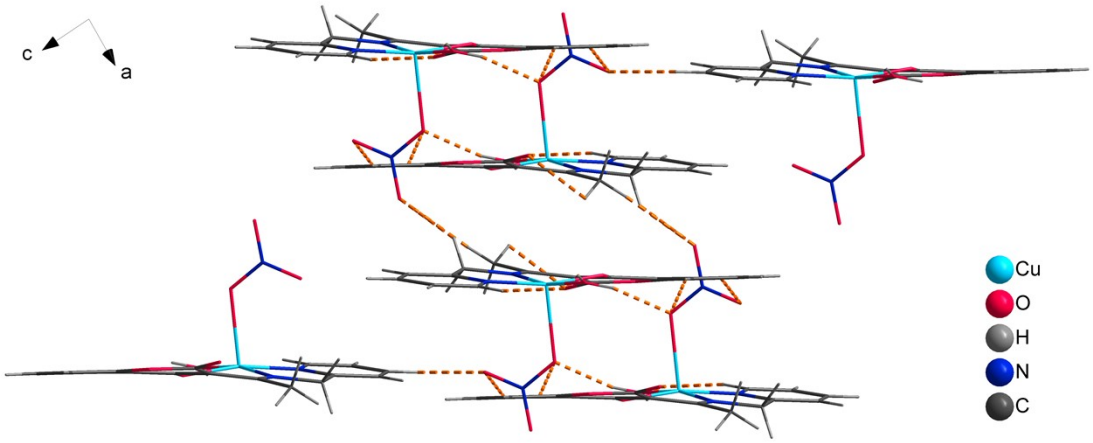

Figure S6. Part of the 3D structure of **5** caused by classical and non-classical hydrogen bonds shown as orange dashed lines.

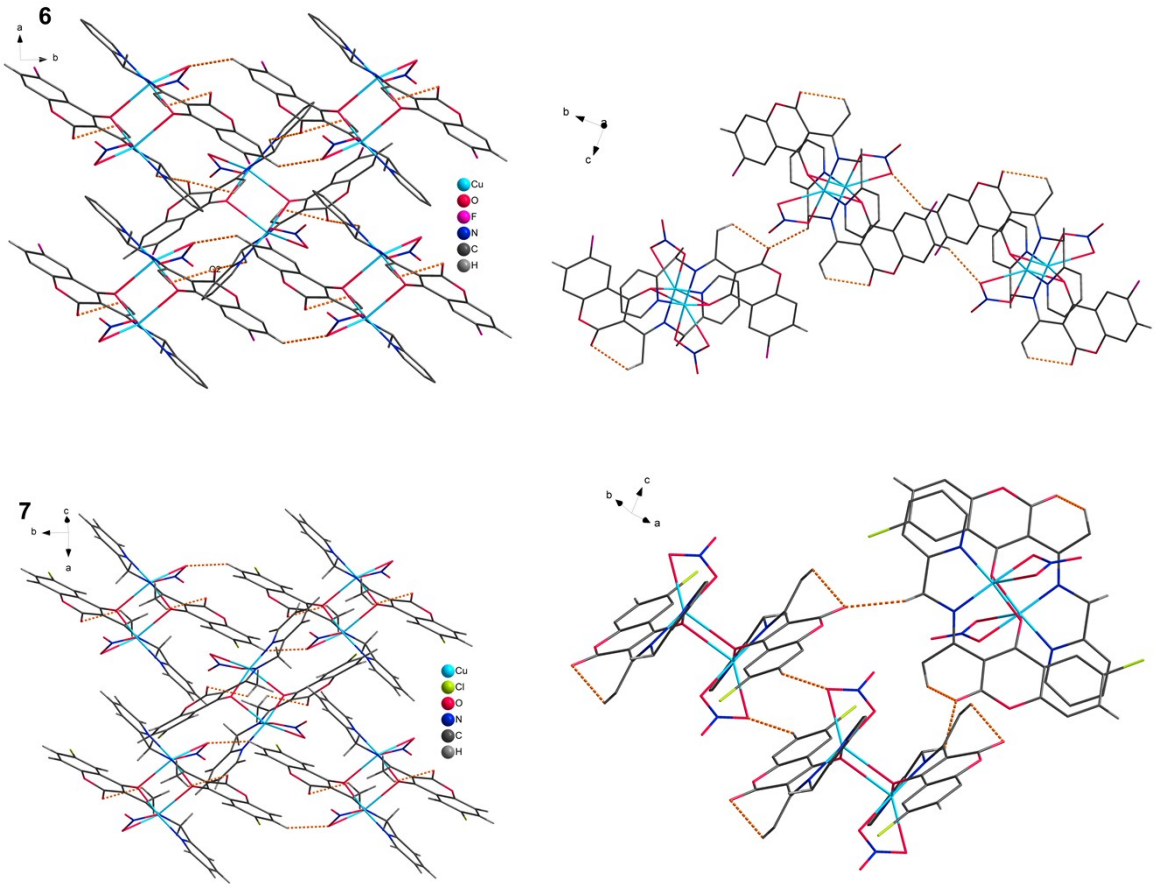

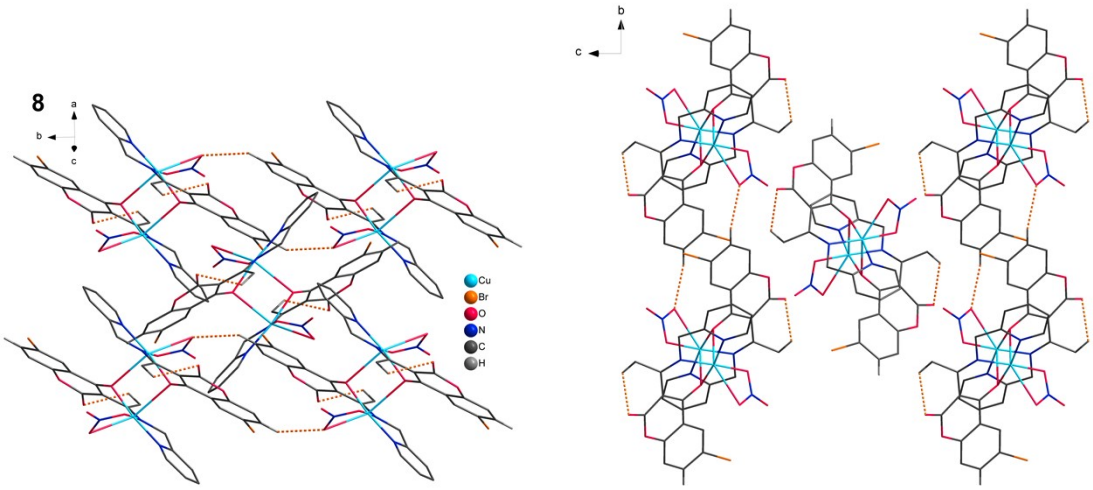

Figure S7. Part of 3D structures of **6-8** caused by non-classical hydrogen bonds (orange dashed lines) showed in different viewing directions, hydrogen atoms not involved in hydrogen bonds are for clarity reasons not illustrated.

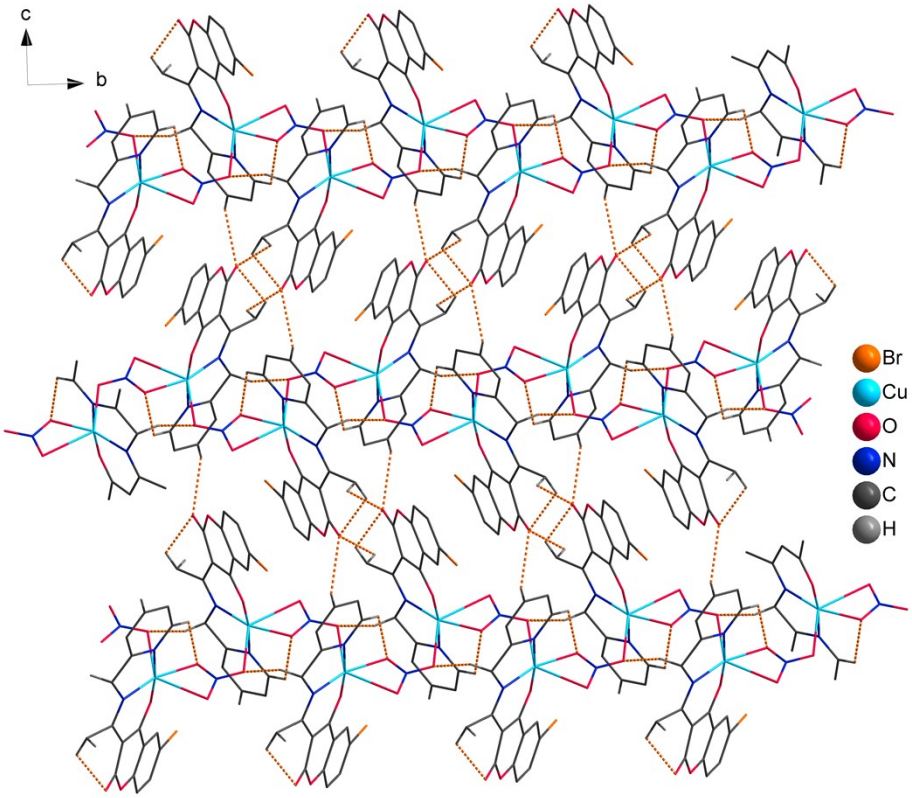

Figure S8. Part of the 2D structure of **9** caused by non-classical hydrogen bonds shown as orange dashed lines.

Table S4. Comparison of the Hirshfeld surface coverage by close contacts of respective types for complexes **5**–**9**.

short contact	Cu···O/O···Cu [%]	H···O/O···H [%]	H···X/X···H [%]	C···C [%]	H···H [%]	H···C/C···H [%]
5	0.3	35.6	-	5.4	32.7	13.7
6	2.0	29.1	9.5	8.0	25.2	9.0
7	2.0	28.7	11.2	7.2	23.5	9.9
8	2.0	28.8	11.8	6.9	23.0	10.0
9	2.4	27.0	9.1	4.5	22.2	17.8

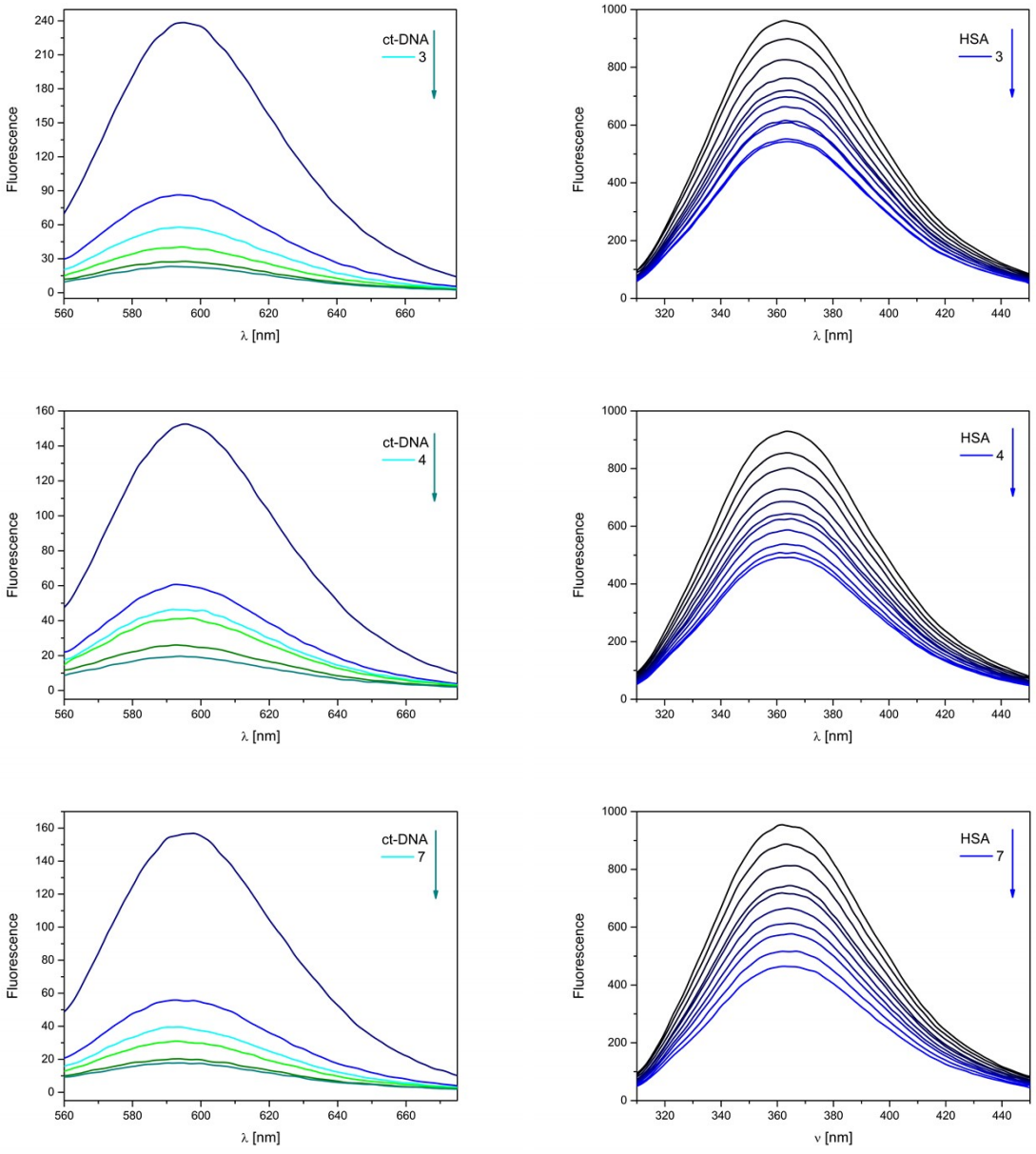

Figure S9. Fluorescence emission spectra of ct-DNA-EB complex (λ_{ex} = 520 nm) upon gradual addition of studied complexes **3**, **4** and **7** in the concentration range 0 – 5 μM (left) and fluorescence emission spectra of HSA (λ_{ex} = 295 nm) upon addition of complexes **3**, **4** and **7** (right).

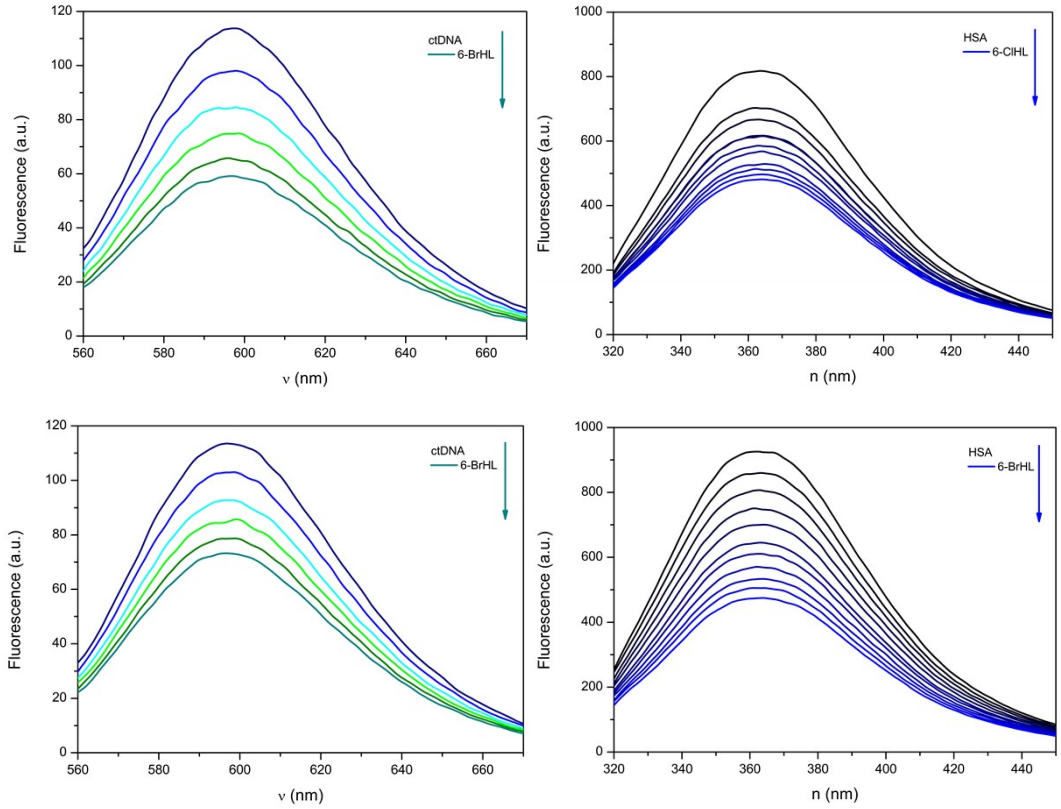

Figure S10. Fluorescence emission spectra of ct-DNA-EB complex (λ_{ex} = 520 nm) upon gradual addition of studied compounds **6-ClHL** and **6-BrHL** in the concentration range 0 – 25 μM (left) and fluorescence emission spectra of HSA (λ_{ex} = 295 nm) upon addition of compounds **6-ClHL** and **6-BrHL** (right).

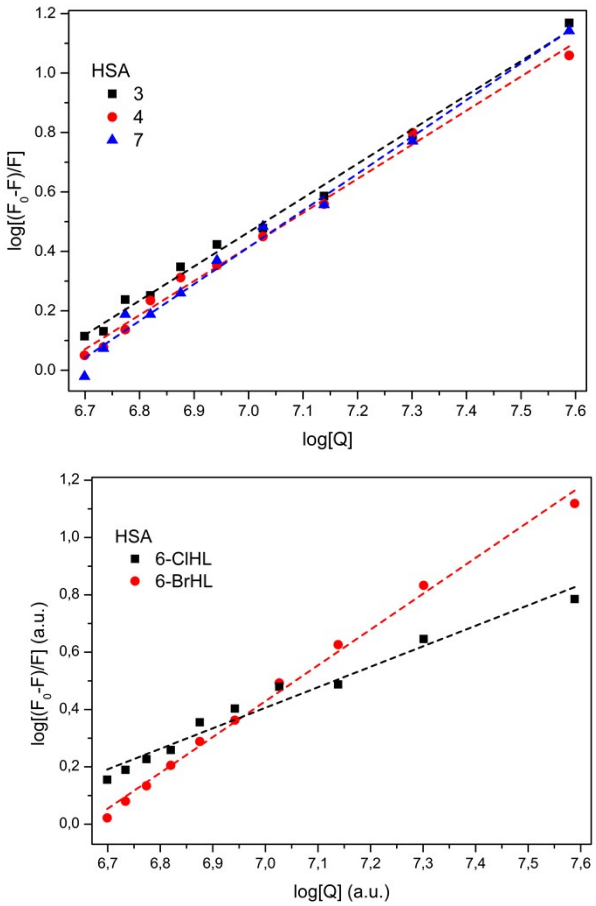

Figure S11. Logarithmic plots of HSA binding of the complexes **3**, **4, 7,** and the ligands **6-ClHL** and **6-BrHL** .

Table S5. Percentage of DPPH radical scavenging activity of prepared compounds **3**, **4** and **7**.

***c* [μM]**	***Q* [%]**		
	3	**4**	**7**
0	0	0	0
50	2.648	3.259	4.277
100	7.943	6.823	8.350
150	12.831	9.369	19.043
200	17.210	12.118	25.662

References

1. CrysAlisPRO, Version 1.0.43, Oxford Diffraction /Agilent Technologies UK Ltd, Yarnton (England) 2020.

2. Sheldrick GM. *SHELXT* – Integrated space-group and crystal-structure determination. Acta Crystallogr A Found Adv. 2015 Jan 1;71(1):3–8.

3. Sheldrick GM. Crystal structure refinement with *SHELXL*. Acta Crystallogr C Struct Chem. 2015 Jan 1;71(1):3–8.

4. Farrugia LJ. *WinGX* and *ORTEP for Windows* : an update. J Appl Crystallogr. 2012 Aug 1;45(4):849–54.

5. Spek AL. Structure validation in chemical crystallography. Acta Crystallogr D Biol Crystallogr. 2009 Feb 1;65(2):148–55.

6. K. Brandenburg, DIAMOND, Version 3.2k, Crystal Impact GbR, Bonn (Germany) 2014.

7. Spackman PR, Turner MJ, McKinnon JJ, Wolff SK, Grimwood DJ, Jayatilaka D, et al. *CrystalExplorer* : a program for Hirshfeld surface analysis, visualization and quantitative analysis of molecular crystals. J Appl Crystallogr. 2021 June 1;54(3):1006–11.

8. Gold V, editor. The IUPAC Compendium of Chemical Terminology: The Gold Book [Internet]. 4th edn. Research Triangle Park, NC: International Union of Pure and Applied Chemistry (IUPAC); 2019. Available from: https://goldbook.iupac.org/